Available online at www.sciencedirect.com
SCIENCE DIRECT
ELSEVIER
European Journal of Mechanics B/Fluids 24 (2005) 125–136
EUROPEAN JOURNAL OF MECHANICS B/FLUIDS

Orientation statistics and effective viscosity of suspensions of elongated particles in simple shear flow

C. Pozrikidis *

Department of Mechanical and Aerospace Engineering, University of California, San Diego, La Jolla, CA 92093-0411, USA

Received 23 September 2003; received in revised form 20 February 2004; accepted 17 July 2004

Available online 11 September 2004

Abstract

The significance of the particle aspect ratio on the statistics of the particle orientation and effective viscosity of a non-dilute suspension in simple shear flow is discussed and investigated by dynamical simulation. It is argued that, in the absence of an imposed length scale or screening dimension due to bounding surfaces, assumed periodicity, or long-range particle interactions, the concept of rotational diffusivity is not appropriate in the limit of infinite dilution for non-colloidal systems. Numerical simulations are carried out based on an improved implementation of the boundary-element method for particulate Stokes flow, featuring the iterative solution of the master linear system for the particle contour traction and particle linear and angular velocities, based on particle-cloud clustering. The numerical results confirm that the transition from a nearly-ordered to the random state due to particle interactions occurs on a time scale that is consistent with the theoretical estimate, and demonstrate that the particle eccentricity reduces the effective viscosity of the suspension and skews the orientation probability density distribution in the direction of the unperturbed shear flow.

Keywords: Suspensions; Orientation pdf; Effective viscosity; Boundary-Element Methods

1. Introduction

The rheological properties and dynamics of the microstructure of suspensions of spherical particles in viscous flow have been studied extensively by experiment, theory, and numerical simulation (e.g., [1–3]). In contrast, investigations of suspensions of non-spherical particles have been limited to the computation of the resistance and mobility tensors in infinite and wall-bounded flow, illustration of single particle trajectories, estimation of the rheological properties in the limit of infinite dilution, and analysis of the statistical properties of semi-dilute systems involving liquid crystals and elongated fibers resembling rods (e.g., [4,5]). Numerical simulations of the hydrodynamics of fiber suspensions have been pursued by several authors under simplifying assumptions regarding the fiber constitution, the inter-particle hydrodynamic interactions, the nature of the particle mechanical contact, and the particle spatial and orientational distribution (e.g., [6–8]). The pervasiveness of elongated and irregularly shaped particles in various engineering and biophysical applications involving fiber-reinforced materials, liquid crystals, macromolecules and proteins, underscores the need for further investigation.

* Tel.: +1-858-534-6530; fax: +1-858-534-7078.
E-mail address: cpozrikidis@ucsd.edu (C. Pozrikidis).

0997-7546/$ – see front matter
doi:10.1016/j.euromechflu.2004.07.003

Of particular interest in this work is the effect of the particle shape and aspect ratio on the effective viscosity of a suspension, and the significance of inter-particle interactions on the particle orientation probability density function (opdf). Although microstructural models of fiber suspensions are available, the theory relies on an assumed effective hydrodynamic rotational diffusivity for the opdf whose existence for non-Brownian systems has not been rigorously established. More important, phenomenological closure is required to obtain a self-contained system of governing equations.

In this article, we make two contributions to the theoretical analysis of non-dilute suspensions of elongated particles in simple shear flow. First, the dispersion in orientation space is discussed for two- and three-dimensional systems in the limit of infinite dilution, and it is argued that, although the concept of orientational self-diffusivity is not appropriate in the absence of an imposed length scale or screening dimension, a time scale over which an initially nearly ordered system undergoes transition to the random state can be deduced from first principles. Second, numerical simulations are carried out to confirm the theoretical prediction and illustrate the effect of the particle aspect ratio and areal fraction for an idealized two-dimensional system. The simulations rely on an efficient implementation of the boundary-element method, wherein the master linear system for the particle-contour traction and particle translation and rotational velocities is solved by a new iterative method based on particle-cloud clustering. The numerical results illustrate the effect of the suspension areal fraction and particle aspect ratio on the suspension effective viscosity and on the orientation probability density function with reference to a possible nematic transition.

2. Orientational dispersion of a dilute suspension

Consider the flow of an idealized two-dimensional, dilute suspension of neutrally-buoyant and torque-free rigid particles undergoing simple shear flow along the x axis, as illustrated in Fig. 1. Under the influence of the shear flow, the particles translate and rotate about their designated centers, exhibiting a nearly periodic motion. As long as the particle number density is non-zero, however small, one particle occasionally intercepts another particle in the evolving suspension. Assuming, as a first approximation, that both particles are advected along the x axis with the velocity of the unperturbed flow, we find that the rate of interception of a test particle whose center is located at y with another particle whose center lies inside a horizontal strip of width $\mathrm{d}y'$ centered at y' is

$$r(y, y') = k|\delta y| n(y'), \tag{1}$$

where k is the shear rate of the unperturbed flow, $\delta y \equiv y - y'$ is the particle separation before interception, and n is the particle number density, defined as the number of particles per unit area of the suspension. For simplicity, we have assumed that n is only a function of position normal to the direction of the shear flow. The pairwise interceptions disturb the angular velocity of rotation of the test particle and cause a net shift in the particle orientation after separation, denoted by $\Delta\theta$. The sign and magnitude of $\Delta\theta$ depend on the relative particle position and orientation before interception.

In the case of circular particles, because interception always delays the rotation, $\Delta\theta$ is a positive and even function of the particle separation before interception, δy. Furthermore, because the particles are assumed torque-free and neutrally buoyant, at large separations, δy, the perturbation flow at the location of a test particle due to an intercepting particle behaves like the flow due to a stresslet, and thus decays like $ka/|\delta y|$, where a is the particle radius, related to the particle number density and

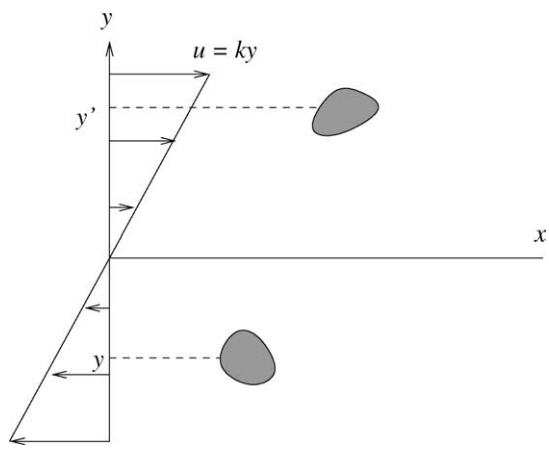

Fig. 1. Schematic illustration of a two-dimensional suspension undergoing simple shear flow.

areal fraction by $\phi = n\pi a^2$ (e.g., [10]). Correspondingly, the perturbation in the velocity gradient tensor at the location of the test particle decays like $k(a/|\delta y|)^2$, and the tail-end of the net shift in the particle orientation behaves like

$$\Delta\theta \sim \pi\left(\frac{a}{|\delta y|}\right)^2. \tag{2}$$

When the particle density distribution is uniform over a region that is large compared to the particle size, a particle will experience a large number of interceptions while remaining in an essentially unchanged environment. Under the fundamental assumption that the interceptions are uncorrelated, we may attempt to use the theory of random walks to describe the evolution of the particle orientation in terms of a long-time orientational self-diffusivity D_o, defined as

$$D_o = \int_a^\infty [\Delta\theta - \overline{\Delta\theta}\,]^2 r(y, y')\,\mathrm{d}\delta y, \tag{3}$$

where $\overline{\Delta\theta}$ is the mean value,

$$\overline{\Delta\theta} = \int_a^\infty \Delta\theta r(y, y')\,\mathrm{d}\delta y. \tag{4}$$

Unfortunately, substituting (1) in (4), and using the asymptotic estimate (2), we obtain an integrand that behaves like $1/|\delta y|$, yielding an improper integral for $\overline{\Delta\theta}$. This divergence suggests that the perturbations in orientation space are non-diffusive, and therefore the evolution of the orientation probability density function (opdf) may not be described by the Smoluchowski equation in the limit of infinite dilution (e.g., [9], p. 294). Moreover, the divergence of the integral in (4) underscores the importance of an external length scale associated with the finite dimension of the flow boundaries, an assumed periodicity, or an internal length scale associated with a "screening length" in a semi-dilute suspension. The latter is defined as the distance over which hydrodynamic perturbations effectively vanish through a cloud of surrounding particles.

In spite of the improper nature of the mean-value integral in the limit of infinite dilution, a time scale, τ, over which random perturbations cause the effect of the initial condition to disappear can be defined in terms of the unshifted variance,

$$\frac{1}{\tau} \equiv \int_a^\infty \Delta\theta^2 r(y, y')\,\mathrm{d}\delta y \sim kn\pi^2 a^4 \int_a^\infty \frac{\mathrm{d}\delta y}{|\delta y|^3} \sim \frac{\pi^2}{2} kna^2 = \frac{\pi}{2}\phi k. \tag{5}$$

Rearranging, we find

$$\tau \sim \frac{2}{\pi\phi k}. \tag{6}$$

Given the existence of the unshifted variance integral, a method by which the shifted variance (3) can be renormalized is not apparent.

The preceding analysis can be repeated for the lateral and longitudinal particle self-diffusivities, defined in terms of the respective net particle displacements after interception, Δx and Δy, both regarded as functions of the lateral particle separation before interception, δy. In the case of circular particles, reversibility of Stokes flow requires that $\Delta y = 0$ for any δy. Thus, the corresponding self-diffusivity is due to multi-particle interceptions. On the other hand, because Δx is an odd function of δy, the corresponding mean value $\bar{\Delta} x$ is zero. However, because Δx decays like $a/\delta y$ in accord with the aforementioned velocity field due to a stresslet (e.g., [10]), the longitudinal diffusivity integral is divergent.

The counterpart of (4) for a three-dimensional suspension of spherical particles of radius a undergoing shear flow along the x axis, is

$$\overline{\Delta\theta} = \int_a^\infty\int_a^\infty \Delta\theta r(y, y')\,\mathrm{d}\delta y\,\mathrm{d}\delta z, \tag{7}$$

where δz is defined by analogy with δy. Far from a test particle, as $\delta r \equiv (\delta y^2 + \delta z^2)^{1/2} \to \infty$, the velocity gradient tensor behaves like that induced by a three-dimensional stresslet; accordingly, $\Delta\theta \sim (a/\delta r)^3$, and the integral in (7) is divergent. On the other hand, the lateral and longitudinal diffusivity integrals are both convergent.

3. Numerical simulations

To provide support for the theoretical prediction (6) and also illustrate the effect of the particle aspect ratio, we consider the shear flow of an idealized doubly periodic suspension of two-dimensional, circular or elliptical rigid particles suspended in a Newtonian fluid, and study the particle motion by dynamical simulation. At the origin of computational time, the suspension is subjected to a simple shear flow, whereupon the particles start translating and rotating about their centers with appropriate linear and angular velocities, as required by the condition of vanishing force and torque.

The evolving structure of the doubly periodic suspension is defined by two base vectors. The first base vector is oriented along the x axis and remains constant in time, while the second base vector is convected as though it were a material line, under the influence of the shear flow. At the initial instant, the base vectors describe a square lattice with side length L, and the areal fraction of the particles is $\phi = N_p A_p / L^2$, where A_p is the area of each particle, and N_p is the number of particles in each periodic cell. We shall assume that the Reynolds number of the flow past each particle is so small that the motion of the fluid is governed by the linear equations of Stokes flow [10].

To compute the motion of the particles, we solve an integral equation of the first kind for the traction distribution along the particle contours, $\mathbf{f} = \boldsymbol{\sigma} \cdot \mathbf{n}$, where $\boldsymbol{\sigma}$ is the stress tensor, and $\mathbf{n}$ is the unit vector normal to the particle contour [10],

$$\frac{1}{4\pi\mu} \int_C G_{ij}(\mathbf{x}, \mathbf{x}_0) f_i(\mathbf{x}) \, \mathrm{d}l(\mathbf{x}) + U_j^{(k)} + \varepsilon_{jzm} \Omega_z^{(k)} \big(\mathbf{x}_0 - \mathbf{x}_c^{(k)}\big)_m = u_j^{\infty}(\mathbf{x}_0). \tag{8}$$

In this equation, the point $\mathbf{x}_0$ is located on the surface of the kth particle, C is the collection of all particle contours, G_{ij} is the doubly periodic Green's function of two-dimensional Stokes flow, $\mathbf{U}^{(k)}$ is the velocity of translation of the kth particle center in the xy plane, $\Omega_z^{(k)}$ is the angular velocity of rotation of the kth particle about the z axis around the particle center, $\mathbf{x}_c^{(k)}$, and $\mathbf{u}_j^{\infty} = (ky, 0)$ is the velocity of the undisturbed shear flow. The ith component of the force and z component of the torque exerted on the kth particle are given, respectively, by

$$F_i^{(k)} = \int_{C_k} f_i(\mathbf{x}) \, \mathrm{d}l(\mathbf{x}), \qquad T_z^{(k)} = \varepsilon_{zlm} \int_{C_k} f_l(\mathbf{x}) \big(\mathbf{x} - \mathbf{x}_c^{(k)}\big)_m \, \mathrm{d}l(\mathbf{x}), \tag{9}$$

for $i = x, y$, where C_k is the kth particle contour. In the case of force-free and torque-free particles presently considered, the left-hand sides of (9) are required to be equal to zero at all times.

Because the traction distribution along each particle contour can be enhanced with an arbitrary multiple of the normal vector, the integral equation (8) does not have a unique solution. One way to circumvent this difficulty is to add to the left-hand side of (8) the deflating term

$$\mathbf{n}(\mathbf{x}_0) \bigg(\int_{C_k} \mathbf{f} \cdot \mathbf{n} \, \mathrm{d}l - \alpha_k \bigg), \tag{10}$$

where α_k is an arbitrary constant, thereby forcing the traction distribution to satisfy the integral constraint $\int_{C_k} \mathbf{f} \cdot \mathbf{n} \, \mathrm{d}l = \alpha_k$. The problem is then reduced to solving the integral equation (8) for the uniquely defined traction, and for the particle linear and angular velocities, while simultaneously satisfying the integral constraints (9). Once the particle velocities are available, the particle positions and inclinations can be advanced in time by integrating the ordinary differential equations

$$\frac{\mathrm{d}\mathbf{x}_c^{(k)}}{\mathrm{d}t} = \mathbf{U}^{(k)}, \qquad \frac{\mathrm{d}\theta^{(k)}}{\mathrm{d}t} = \Omega_z^{(k)}, \tag{11}$$

where $\theta^{(k)}$ is the kth particle inclination.

The solution of the constrained integral equations was computed using an improved version of a boundary-element method developed in earlier work [11,12]. In the present implementation, the traction is assumed to be constant over each boundary element. Boundary collocation is then applied to obtain the master linear system

$$\mathbf{A} \cdot \mathbf{z} = \mathbf{b}, \tag{12}$$

where $\mathbf{A}$ is the master influence matrix (MIM). The solution vector $\mathbf{z}$ contains the x and y components of the boundary-element tractions, followed by the x and y components of the particle linear velocities, and the z component of the particle angular velocities. In particular, the vector $\mathbf{z}$ is comprised of N_p blocks, where the size of the ith block is $2N_E + 3$, and N_E is the number of boundary elements around the ith particle. The diagonal blocks of $\mathbf{A}$ describe particle self-interaction, and the off-diagonal blocks describe mutual particle interactions. In simulations with 49 particles and 24 boundary elements around each particle contour, the size of the linear system is 2499×2499.

To render the simulations practically feasible, we solve the master linear system using a novel iterative method in which the master influence matrix (MIM) is decomposed into its N_p^2 constituent particle interaction matrices (PIM), denoted by $\boldsymbol{\Phi}_{ij}$, $i, j = 1, \ldots, N_p$. These matrices are computed and stored explicitly by looping over the particles and then over the particle boundary elements twice. By definition, $\boldsymbol{\Phi}_{ii}$ is the particle self-interaction matrix. Next, the neighbors of each particle are identified, and the corresponding self- and mutual-interaction matrices are compiled into particle cloud matrices (PCM), denoted by $\boldsymbol{\Psi}_i$, $i = 1, \ldots, N_p$, where the first diagonal block of $\boldsymbol{\Psi}_i$, is the particle self-interaction matrix, $\boldsymbol{\Phi}_{ii}$. Neighbor identification is done through an association matrix, L_{ij}, defined such that $L_{ij} = 1$ if particles i and j are neighbors, and $L_{ij} = 0$ otherwise [11]. Note that the PCMs of neighboring particles share the corresponding PIMs. Specifically, if two particles form an isolated doublet, the PCMs are composed of four transposed PIMs. Once the PCMs are defined, their inverses are computed and stored to be used in the iterations. In practice, depending on the particle areal fraction, the kth particle cluster involves 1 to 5 particles.

The iterations themselves are based on the repetitive solution of the particle-cloud sub-systems

$$\boldsymbol{\Psi}_i \cdot \check{f}_i = \mathbf{b}_i - \sum_{j=1}^{N_p} \boldsymbol{\Phi}_{ij} \cdot \mathbf{f}_j, \tag{13}$$

for $i = 1, \ldots, N_p$, where $\check{f}_i$ is the solution block corresponding to the ith particle cloud, and $\mathbf{f}_i$ is the solution block for the ith particle. The sum on the right-hand side of (13) is restricted over non-neighbors, that is, over those values of j satisfying $L_{ij} \neq 1$. As soon as the solution of (13) is found, the tractions around the particles participating in the cloud are updated by dismantling the corresponding particle block $\check{f}_i$. The updates are carried out until the error drops to a preset level on the order of 10^{-8} in proper dimensionless units. Typically, 4–10 iterations are required for convergence.

In the numerical simulations presented in the next section, the number of particles distributed over each period is $N_p = 7^2 = 49$, and the number of boundary elements along each particle contour ranges from 16 to 24 depending on the suspension areal fraction and particle aspect ratio. Extensive numerical experimentation has shown that the numerical error has a minor effect on the overall rheological and statistical properties of the suspension. In fact, time sequences presented later in the next section are composed of simulation segments conducted with different levels of discretization. Time integration of the equations governing the particle motion and orientation was carried out using the second-order Runge–Kutta method with a constant time step $\Delta t = 0.02k^{-1}$, where k is the shear rate of the simple shear flow. The most demanding simulations require several days of CPU time of an Intel 2.5 GHz processor running Linux.

The rheological properties of the doubly periodic suspension are described by Batchelor's effective stress tensor [13]

$$\langle \sigma_{ij} \rangle = \sigma_{ij}^{\infty} + \frac{1}{A} \sum_{k=1}^{N_p} \int_{C_k} (f_i x_j + f_j x_i)\, \mathrm{d}l, \tag{14}$$

where σ_{ij}^{∞} is the stress tensor of the unperturbed shear flow, A is the area of a periodic cell, $\mathbf{f}$ is the hydrodynamic traction exerted on the particle surfaces, and C_k is the contour of the kth particle. The second term on the right-hand side of (14) is the "particle stress tensor", $\boldsymbol{\sigma}^P$. The effective viscosity of the suspension is defined as

$$\mu_{\mathrm{Eff}} = \frac{1}{k} \langle \sigma_{xy} \rangle = \mu \left(1 + \frac{1}{\mu k} \sigma_{xy}^P \right). \tag{15}$$

4. Results and discussion

To demonstrate the transition from a nearly ordered to the random state due to hydrodynamic interactions, and also confirm the estimate (6), we consider the evolution of a dilute suspension of elliptical particles with aspect ratio 4, at the low areal fraction $\phi = 0.0154$. At the initial instant, the particle centers are arranged on a randomly perturbed square lattice, with the major particle axis pointing uniformly along the y axis, transversely to the incident shear flow, as shown in Fig. 2(a). If the suspension were infinitely dilute, each particle would execute periodic rotation with a highly fluctuating angular velocity over the time period $T = 26.6k^{-1}$. The simulations suggest that, because of random particle interceptions, the initially nearly uniform spatial particle orientation becomes random after a certain evolution time, while particle doublets and clusters develop, as shown in Fig. 2(b)–(d).

The solid line in Fig. 3(a) describes the evolution of the suspension effective viscosity, μ_{Eff}, reduced by the suspending fluid viscosity, μ. The dotted line describes the effective viscosity of a perfectly ordered suspension where, at the initial instant, the particles are located precisely at the nodes of the unperturbed square lattice, with the major particle axis pointing uniformly in the y direction. The viscosity of the ordered suspension exhibits nearly periodic oscillations with a dominant frequency

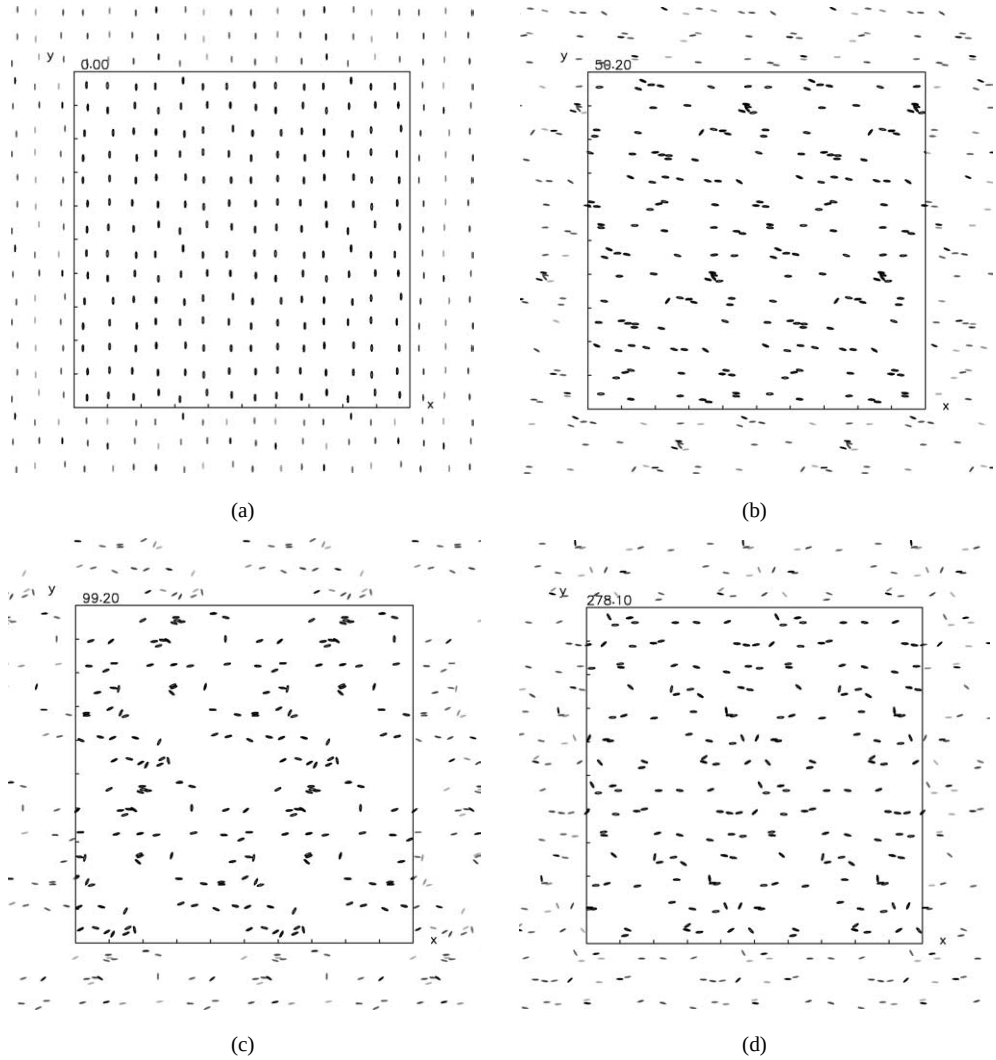

Fig. 2. Evolution of a dilute suspension of elliptical particles with aspect ratio 4, for particle areal fraction $\phi = 0.0154$. At the initial instant, the particles are distributed on a perturbed square lattice with the major particle axis pointing along the y axis, as shown in (a). The geometry of the microstructure at the end of the simulation is shown in (d). The counters above the panels indicate the dimensionless elapsed time kt.

corresponding to half the period of rotation of a solitary particle in simple shear flow, $T/2 \simeq 13.3k^{-1}$. This fundamental frequency is accompanied by subharmonic and superharmonic frequencies arising by hydrodynamic interactions of each particle with overpassing particles in the doubly periodic array. During the initial stages of the motion, the effective viscosity of the random suspension exhibits damped oscillations with period $T/2$. After an evolution time on the order of $\tau = 2/(\pi\phi k) = 41k^{-1}$, the amplitude of the oscillations has decayed to nearly half the initial value, in agreement with the theoretical predictions. In subsequent evolution, the dominant frequency associated with the solitary particle rotation is further attenuated, and the suspension assumes an apparently random state.

To illustrate the transition to the random state in more quantitative terms, we consider the Fourier spectrum of the suspension effective viscosity shifted by the mean value. The Fourier coefficients, $|a_p|$, are computed by applying Fourier decomposition over a time interval of length $2T = 53.2k^{-1}$, starting at kt = 1, 50, 100, 150, 200, and 250, and are then reduced by the pure fluid viscosity. Results are shown in Fig. 3(b) with alternating solid and dashed lines for the random suspension, and with the dotted line for the ordered suspension. The spectrum of the ordered suspension exhibits a high peak at $p = 4$, independent of the period of averaging, corresponding to half the frequency of rotation of a solitary particle in simple shear flow. The spectrum of the random suspension also exhibits a high peak at $p = 4$ during the initial time period, $0 < kt < 53.2$. However, the height of this peak is subsequently reduced, and the energy content of the $p = 4$ mode becomes comparable to that of higher frequencies

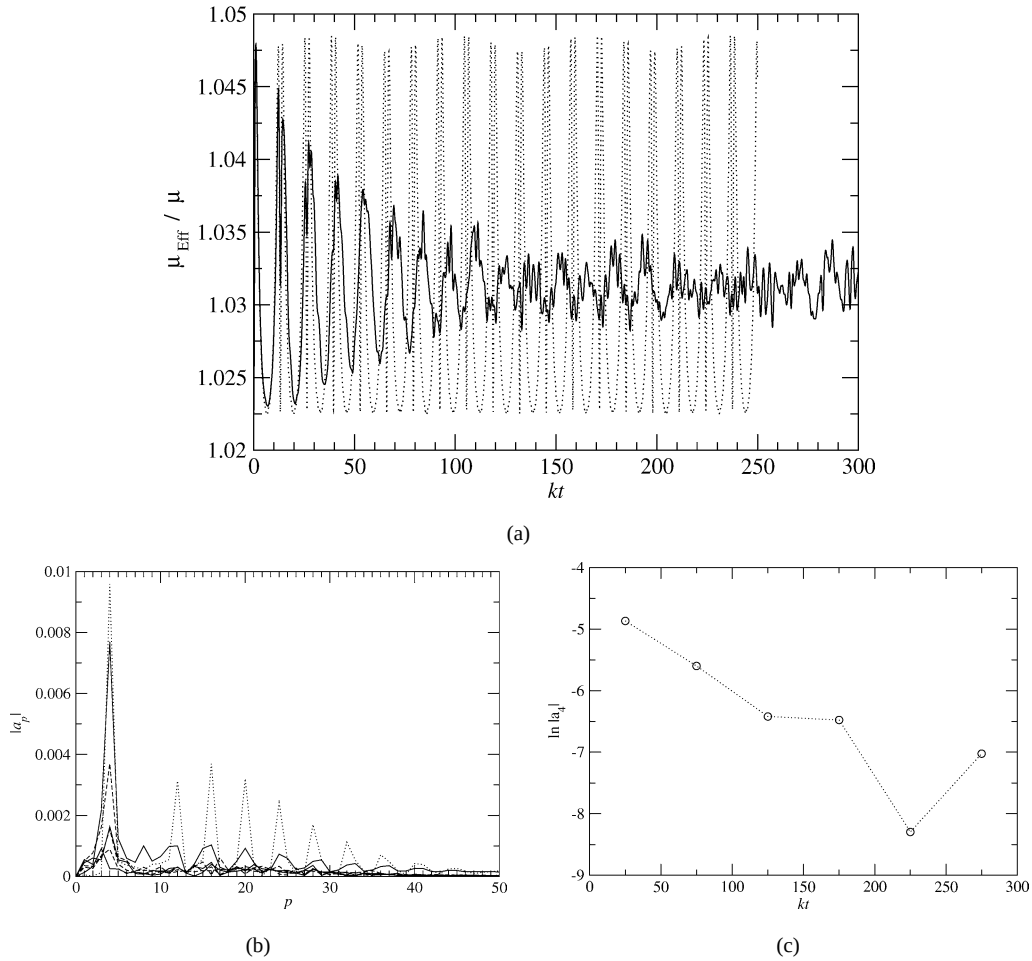

Fig. 3. (a) Evolution of the effective viscosity of the suspension depicted in Fig. 2 (solid lines), and corresponding evolution in the perfectly ordered state (dotted lines). (b) Fourier spectrum of the effective viscosity over successive periods of time showing the attenuation of the fundamental frequency associated with particle rotation in an infinitely dilute suspension. (c) Decay of the amplitude of the fundamental peak.

approximately at $kt > 150$. Fig. 3(c), shows the amplitude of the fundamental peak plotted against the mid-point time of the Fourier interval on a linear-log scale. The results suggest that the peak decays exponentially during the initial stages of the evolution. The estimated rate of decay read off the graph is approximately $5/300$, corresponding to the time scale $60k^{-1}$, which is reasonably close to the theoretical estimate, $\tau = 41k^{-1}$.

To further confirm the theoretical estimate, we consider the evolution of the nearly-ordered suspension under identical conditions, except that the particles are twice as large, corresponding to the four-fold areal fraction $\phi = 0.0616$. Fig. 4(a, b) shows the particle distribution after elapsed times kt = 20.6 and 50.25, and Fig. 4(c) shows the evolution of the suspension effective viscosity throughout the simulation. The dotted line in Fig. 4(c) corresponds to a perfectly ordered suspension with the same volume fraction, where the particle centers are located at the vertices of a deforming lattice. Comparing Fig. 4(c) with Fig. 3(a), we find that the time scale over which the nearly-ordered suspension becomes apparently random is reduced by a factor of 4, which is consistent with the theoretical prediction. Fig. 4(d) displays the Fourier spectrum corresponding to that shown in Fig. 3(b), computed over the same time interval, $2T = 53.2k^{-1}$, starting at kt = 0 (solid line) or 50 (dashed line). The dotted line corresponds to the aforementioned perfectly ordered suspension. Though the results clearly suggest that the transition time is significantly reduced with respect to that of the dilute suspension, extracting the rate of decay is prohibited by the short duration of the transition period.

Having established that particle interactions cause dispersion in orientation space leading to an apparently random state, we proceed to investigate the rheological and statistical properties of the suspension with emphasis on the effect of the particle aspect ratio. To expedite the approach to statistical equilibration, at the initial instant, the particle centers are distributed on a randomly perturbed square lattice, with the major particle axes pointing in unrelated random directions. Fig. 5 shows the

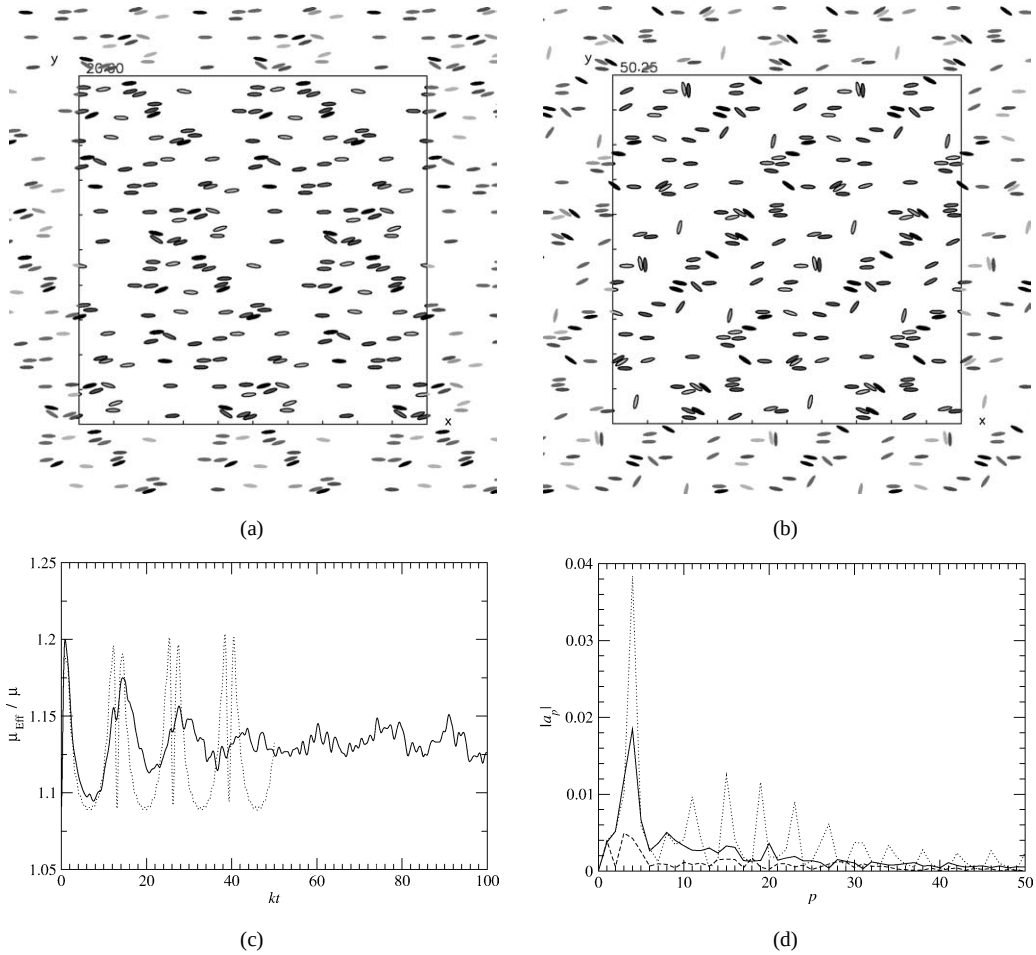

Fig. 4. Evolution of a semi-dilute suspension of elliptical particles with aspect ratio 4, for particle areal fraction $\phi = 0.0616$. At the initial instant, the particles are distributed on a perturbed square lattice with the major particle axis pointing along the y axis, as shown in Fig. 2(a). (c) Evolution of the suspension effective viscosity (solid lines), and corresponding evolution in the perfectly ordered state (dotted lines). (d) Fourier spectrum of the effective viscosity over successive periods of time.

initial and advanced configurations of a suspension of circular and elliptical particles with aspect ratio 4, both for areal fraction $\phi = 0.30$. The spontaneous formation of clusters and chains due to lubrication forces developing between intercepting particles is evident in both cases. The vast majority of the elliptical particles shown on the right of Fig. 5(b) are oriented parallel to the shear flow, as will be further confirmed from examination of the orientation probability density function (opdf).

Fig. 6 illustrates the evolution of the suspension effective viscosity for particle areal fractions $\phi = 0.20$, 0.30, and 0.38, represented by the lowest, middle, and top set of curves. The solid, dotted, and dashed lines correspond, respectively, to particle aspect ratios 1, 2, and 4. In all cases, the suspension effective viscosity increases during the initial transition period due to the spontaneous formation of clusters from initially well-separated particles. Statistical equilibration is established after an evolution time on the order of 10 to 20 inverse shear rates. The viscosity for $\phi = 0.38$ appears to slowly decrease in time after the initial transition period, though the underlying physical reason is not entirely clear. Interestingly, the particle aspect ratio does not seem to have a strong effect on the magnitude of the fluctuations.

Fig. 7 summarizes the dependence of the mean value of the suspension viscosity at equilibration on the particle areal fraction, ϕ, and also demonstrates the effect of the particle aspect ratio. An analytical calculation shows that, in the limit of infinite dilution, the effective viscosity of a suspension of *circular* particles is given by the two-dimensional version of Einstein's law $\mu_{\text{Eff}} = (1 + 2\phi)\mu$ [14]. The results in Fig. 7 show that this theoretical prediction, represented by the solid line, is surprisingly accurate up to moderate areal fractions, $\phi \simeq 0.10$. Given the particle areal fraction, raising the particle eccentricity reduces the suspension effective viscosity. The effect is small for particles with aspect ratio 2, and noticeable for particles with aspect ratio of 4.

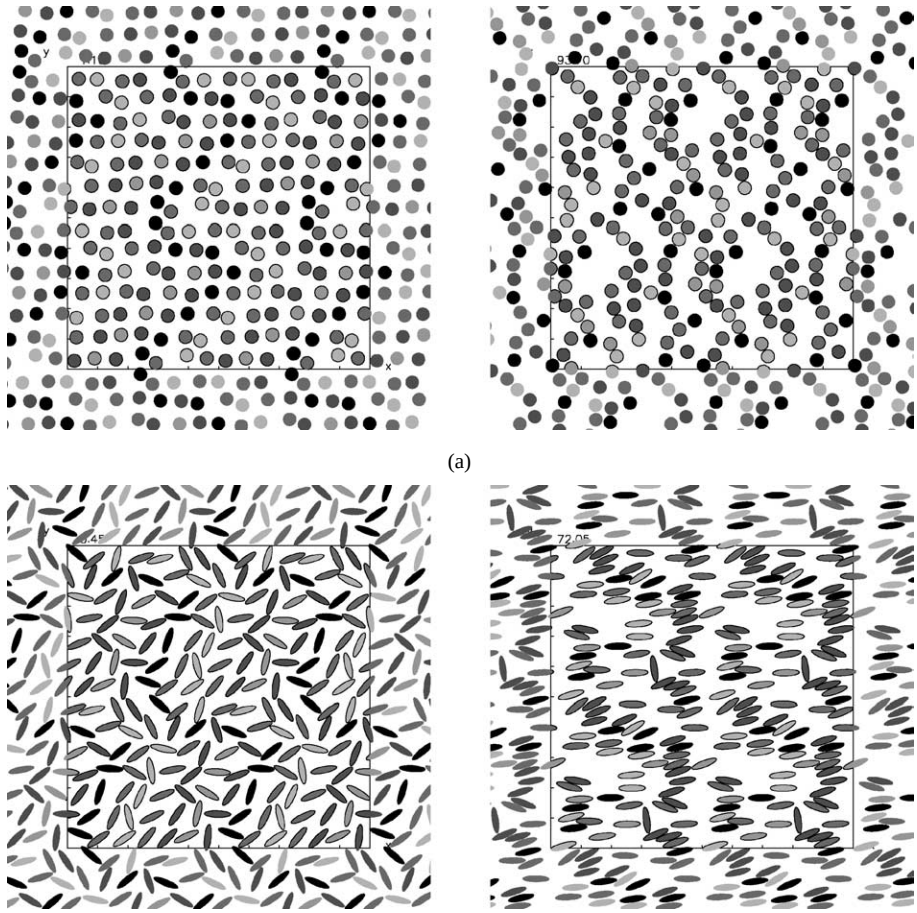

Fig. 5. Initial and advanced configuration of a suspension of (a) circular, and (b) elliptical particles with aspect ratio 4, both at the areal fraction $\phi = 0.30$, subject to simple shear flow in the horizontal direction.

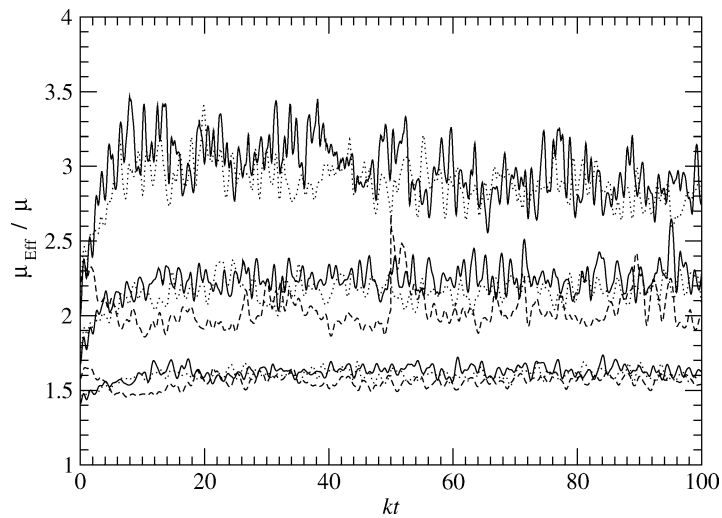

Fig. 6. Evolution of the suspension effective viscosity reduced by the fluid viscosity for particle areal fraction $\phi = 0.20$, 0.30, and 0.38 (lowest, middle, and top set of curves). The solid, dotted, and dashed lines correspond, respectively, to particle aspect ratio 1, 2, and 4.

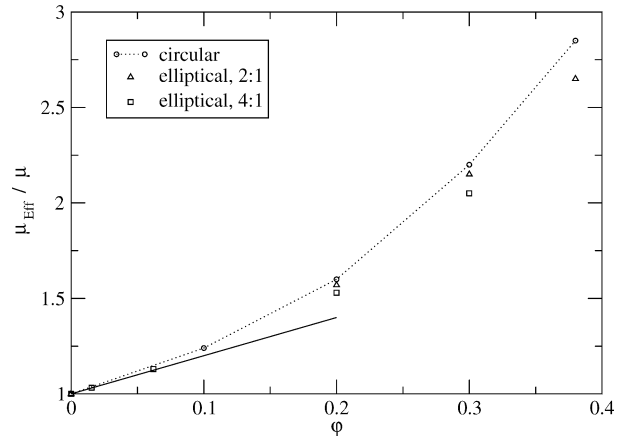

Fig. 7. Dependence of the mean effective suspension viscosity at equilibration on the particle areal fraction and aspect ratio. The solid line represents the theoretical prediction for circular particles in the limit of infinite dilution [14].

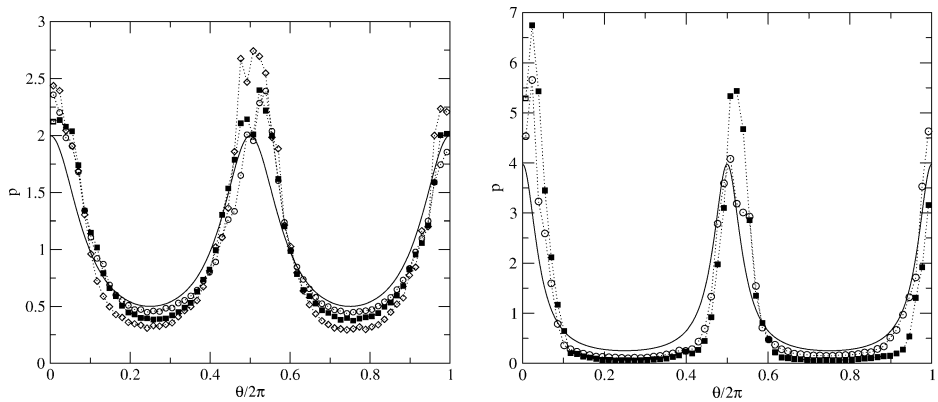

Fig. 8. Orientation pdf (opdf) of elliptical particles with aspect ratio (a) 2, and (b) 4. The smooth solid lines correspond to the limit of infinite dilution; the circles, squares, and diamonds correspond, respectively, to areal fractions $\phi = 0.20$, 0.30, and 0.38.

Of central interest in this work is the effect of the particle aspect ratio and areal fraction on the opdf at statistical equilibration, denoted by $p_o(\theta)$. In the theoretical limit of infinite dilution, particle interactions are negligible to leading-order approximation. At statistical equilibration, $\partial p_o/\partial t = 0$, and the opdf is inversely proportional to the particle angular velocity for each inclination, $\Omega(\theta)$, as required by the conservation law $\partial(\Omega p_o)/\partial\theta = 0$. Physically, the particles spend a longer time at orientations of low angular velocity parallel to the streamlines of the unperturbed shear flow, and a shorter time at orientations of high angular velocity perpendicular to the streamlines of the unperturbed shear flow. In the case of flat plates with infinite aspect ratio, the particles align themselves with the streamlines of the unperturbed shear flow, and p_o reduces to Dirac's delta function centered at the origin. At higher areal fractions, physical exclusion may prevent perfect alignment by interlocking.

Fig. 8 displays the opdf for suspensions of particles with aspect ratio 2 and 4, at several volume fractions. These results were computed by statistical averaging over a period of time spanning from 50 to 100 inverse shear rates after initiation of the motion. The smooth solid lines, corresponding to the limit of infinite dilution, were generated using the method described in the previous paragraph. The circles, squares, and diamonds correspond to areal fractions ϕ = 0.20, 0.30, and 0.38. The results demonstrate that, as particle interactions become stronger at higher areal fractions, the particles are more likely to be oriented in the direction of the shear flow rather than in the normal direction. Physically, particle interception causes the formation of elongated particle doublets that tend to align with the streamlines of the incident flow. The effect is amplified by physical exclusion prohibiting particles from executing complete orbits, as can be seen in Fig. 5(b). In principle, physical exclusion at high areal fractions may cause a transition to the nematic state of liquid crystals, in which the particle centers are distributed randomly in space, while the particle orientation lies within a narrow window [5]. The results shown in Fig. 8 suggest that this transition occurs gradually rather than abruptly at a critical areal fraction in the range of areal fractions considered.

5. Concluding remarks

We have presented theoretical arguments that cast a shadow of doubt on the concept of non-Brownian, hydrodynamically induced rotational diffusivity for dilute suspensions in the absence of a screening length. In contrast, when the perturbations in orientation space are due to Brownian motion in colloidal systems, the fluctuations are undoubtedly diffusive (e.g., [15]). Previous authors have assumed that the evolution of the particle orientation is governed by the Langevin equation forced by a random field due to hydrodynamic interactions resembling white noise, and postulated the existence of a rotational diffusivity in semi-dilute and dense suspensions. Estimates for this diffusivity were obtained by fitting the results of numerical simulations to the predictions of Smoluchowski's equation at statistical equilibration [4]. The arguments put forth in Section 2 underscore the importance of a critical re-examination of the conditions under which the fundamental assumption of diffusive behavior in orientation space is appropriate.

We have carried out numerical simulations to illustrate the effect of particle aspect ratio on the effective viscosity of the suspension and on the orientation probability density function at equilibration. Results on the former confirmed that, given the particle areal fraction, the effective viscosity decreases as the particles become more elongated, over a broad range of areal fractions. Results on the latter suggested that transition to the nematic state is expected to occur gradually rather than abruptly at a critical areal fraction.

Numerical results for the effective viscosity of suspensions of spheroidal particles and cylindrical fibers were presented, respectively, by Claeys and Brady [16] and Mackaplow and Shaqfeh [17]. In both theoretical models, the spatial distribution of the particles is assumed as uniform or isotropic, rather than spontaneously established in the course of a dynamical simulation. The results of Claeys and Brady [16] on the effective suspension viscosity of isotropic dispersions of particles with moderate aspect ratio are consistent with those presented in Fig. 7 of this article. For example, for spheroidal particles with aspect ratio 3, Claeys and Brady [16] find that the reduced effective viscosity μ_{Eff}/μ is approximately 1.75 at particle volume fraction $\phi = 0.2$, and 2.3 at $\phi = 0.3$. However, in contrast with the results shown in Fig. 7, the viscosity of the isotropic dispersion was found to rapidly increase as the particle aspect ratio is raised. Mackaplow and Shaqfeh [17] find that the effective viscosity of a suspension of cylindrical fibers nearly doubles when the fiber volume fraction is 0.05, in agreement with experimental measurements, and discuss possible sources of disagreement with the results of Claeys and Brady's [16], which predict a milder trend. These differences underscore the importance of the particle orientation distribution and the subtle effect of particle interactions in an evolving suspension.

Current efforts are directed toward extending the simulation methods to three-dimensional flow, and investigating the properties of suspensions of elongated spheroidal particles. The insights on computational and physical issues extracted from the present work will serve as a guide in these future endeavors.

Acknowledgements

I am grateful to Anjani Didwania for insightful comments on the manuscript. This research has been supported by a grant provided by the National Science Foundation.

References

[1] R.R. Huilgol, N. Phan-Thien, Fluid Mechanics of Viscoelasticity, Elsevier, Amsterdam, 1997.
[2] D.I. Dratler, W.R. Schowalter, Dynamic simulation of suspensions of non-Brownian hard spheres, J. Fluid Mech. 325 (1996) 53–77.
[3] D.I. Dratler, W.R. Schowalter, R.L. Hoffman, Dynamic simulation of shear thickening in concentrated colloidal suspensions, J. Fluid Mech. 353 (1997) 1–30.
[4] N. Phan-Thien, X.-J. Fan, R.I. Tanner, R. Zheng, Folgar–Tucker constant for a fibre suspension in a Newtonian fluid, J. Non-Newt. Fluid Mech. 103 (2002) 251–260.
[5] S. Chandrasekhar, Liquid Crystals, Cambridge University Press, Cambridge, 1992.
[6] J.E. Butler, E.S.G. Shaqfeh, Dynamic simulations of the inhomogeneous sedimentation of rigid fibres, J. Fluid Mech. 468 (2002) 205–237.
[7] L.H. Switzer, D.J. Klingenberg, Flocculation in simulations of sheared fiber suspensions, Int. J. Multiphase Flow 30 (2004) 67–87.
[8] L. Jianzhong, Z. Weifeng, Y. Zhaosheng, Numerical research on the orientation distribution of fibers immersed in laminar and turbulent pile flows, Aerosol Science 35 (2004) 63–82.
[9] M. Doi, S.F. Edwards, The Theory of Polymer Dynamics, Oxford University Press, New York, 1986.
[10] C. Pozrikidis, Boundary Integral and Singularity Methods for Linearized Viscous Flow, Cambridge University Press, Cambridge, 1992.
[11] C. Pozrikidis, Dynamical simulation of the flow of suspensions of particles with arbitrary shapes, Eng. Anal. Bound. Elem. 25 (2000) 19–30.
[12] C. Pozrikidis, Dynamical simulation of the flow of suspensions: wall-bounded and pressure-driven channel flow, Ind. Eng. Chem. Res. 41 (2002) 6312–6322.

[13] G.K. Batchelor, The stress system in a suspension of force-free particles, J. Fluid Mech. 41 (1970) 545–570.
[14] M. Belzons, R. Blanc, J.-L. Bouillot, C. Camoin, Viscosité d'une suspension diluée et bidimensionnelle de sphères, C. R. Acad. Sci. Paris, Sér. II 292 (1989) 939–944.
[15] L.G. Leal, E.J. Hinch, The effect of weak Brownian rotations on particles in shear flow, J. Fluid Mech. 46 (1971) 685–703.
[16] I.L. Claeys, J.F. Brady, Suspensions of prolate spheroids in Stokes flow. Part 2. Statistically homogeneous dispersions, J. Fluid Mech. 251 (1993) 443–477.
[17] M.B. Mackaplow, E.S.G. Shaqfeh, A numerical study of the rheological properties of suspensions or rigid, non-Brownian fibres, J. Fluid Mech. 329 (1996) 155–186.